We are IntechOpen, the world's leading publisher of Open Access books
Built by scientists, for scientists

6,900
Open access books available

185,000
International authors and editors

200M
Downloads

154
Countries delivered to

Our authors are among the

TOP 1%
most cited scientists

12.2%
Contributors from top 500 universities

CLARIVATE ANALYTICS
BOOK CITATION INDEX
INDEXED

WEB OF SCIENCE™

Selection of our books indexed in the Book Citation Index
in Web of Science™ Core Collection (BKCI)

Interested in publishing with us?
Contact book.department@intechopen.com

Numbers displayed above are based on latest data collected.
For more information visit www.intechopen.com

Failure Mechanism and Property Modification of Insulation Material Used in Inverter-Fed Motors

Yan Yang and Guangning Wu

Abstract

The insulation system of inverter-fed motors is subjected to repetitive impulse voltages, which are generated by pulse width modulation (PWM) converters, and is expected to withstand partial discharge (PD) activity during service. PD-induced dielectric breakdown becomes one of the most important reasons for premature failures of motor insulation. Therefore, the dielectric properties of insulation material used in inverter-fed motors need to be improved to meet the requirement for rapid development of applications. Many approaches have been proposed to improve dielectric properties of insulation material used in inverter-fed motors. In this chapter, we will discuss the failure mechanism, modification approaches, and their effects on dielectric properties of insulation material of inverter-fed motors.

Keywords: inverter-fed motors, insulation material, failure mechanism, modification

1. Introduction

The insulation system of inverter-fed motors is subjected to repetitive impulse voltages that are generated by pulse width modulation (PWM) converters. For high-voltage motors with the rated voltage value greater than 700 V, which also be called as Type II motors, partial discharges (PD) may occur in all insulation systems during operation, but breakdown due to high-voltage endurance may not occur. The insulation materials are expected to withstand partial discharge (PD) activity during service. Under repetitive impulse voltages, accelerating of insulation deterioration would be caused [1]. PD-induced dielectric breakdown is one of the most important reasons for premature failures of motor insulation [2, 3]. In inverter-fed motors, most insulation failures are originated from the non-homogeneous distribution of voltage along the stator windings and are closely related with the short rise time and high frequency of the repetitive impulse voltages [4].

Polyimide (PI) is used as an insulating material for turn-to-turn insulation of inverter-fed traction motors because of its excellent electrical, thermal, and mechanical characteristics [1, 5]. Therefore, the dielectric properties of PI films still need to be improved to meet the requirement for rapid development of industry application [6, 7], especially for PD-dependent lifetime under repetitive impulse voltages. Many approaches have been proposed to improve PD-dependent lifetime of

PI films. One effective approach is synthesizing PI/inorganic nanocomposites [8–11]. Polymer nanocomposites consisting of nanoparticles allow for a large tunability of the dielectric properties by varying the identity and content of nanoadditives. Moreover, lifetime under repetitive impulse voltages is much more closely related to the surface characteristics of PI films, for the degradation is always initiated from surface partial discharge, which is mainly caused by surface charge accumulation and local field enhancement, due to the mismatching of surface charge dissipation and voltage reversion [12–14]. Therefore, surface modification would be another effective approach to improve the lifetime of PI films under repetitive impulse voltages, by modifying the surface characteristics.

To provide a comprehensive understanding to this topic and to clarify the emerging problems, we review the recent progress in the failure mechanism and property modification of insulation material used in inverter-fed motors. Particular attention is paid on PD-dependent lifetime improvement under repetitive impulse voltages of PI films.

2. Failure mechanism of insulation material used in inverter-fed motors

2.1 Electrical stresses in inverter-fed motors

A typical schematic diagram and output waveform of inverter-fed traction motors used in high-speed railways are shown in **Figure 1** [5]. Different from traditional alternating current (AC) motors stressed by the sinusoidal (50 or 60 Hz) voltages, the insulation systems of inverter-fed motors are exposed to transient surge voltages with steep fronts generated by the switching of insulated gate bipolar transistor (IGBT) [6]. Besides, there are other factors that cause PDs, including overvoltage caused by impedance mismatch (between supply cable and motor) and uneven potential distribution could induce partial discharge (PD) in stator
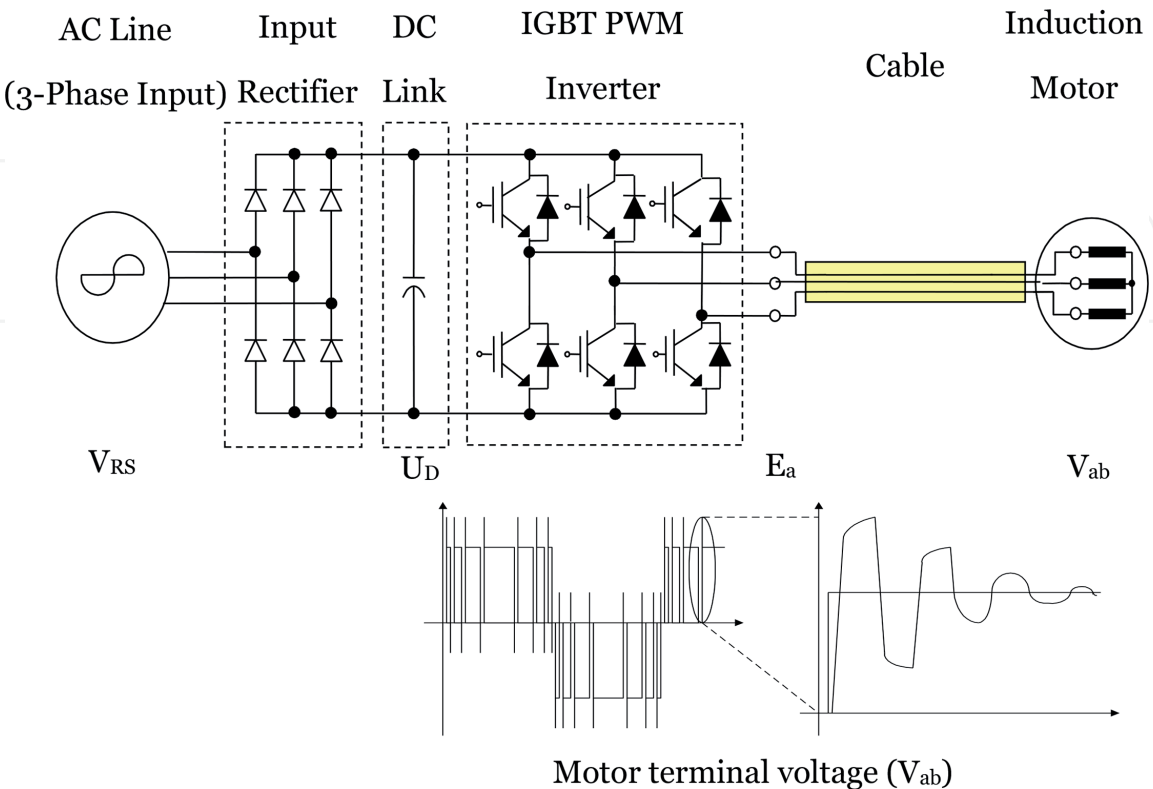

Figure 1.
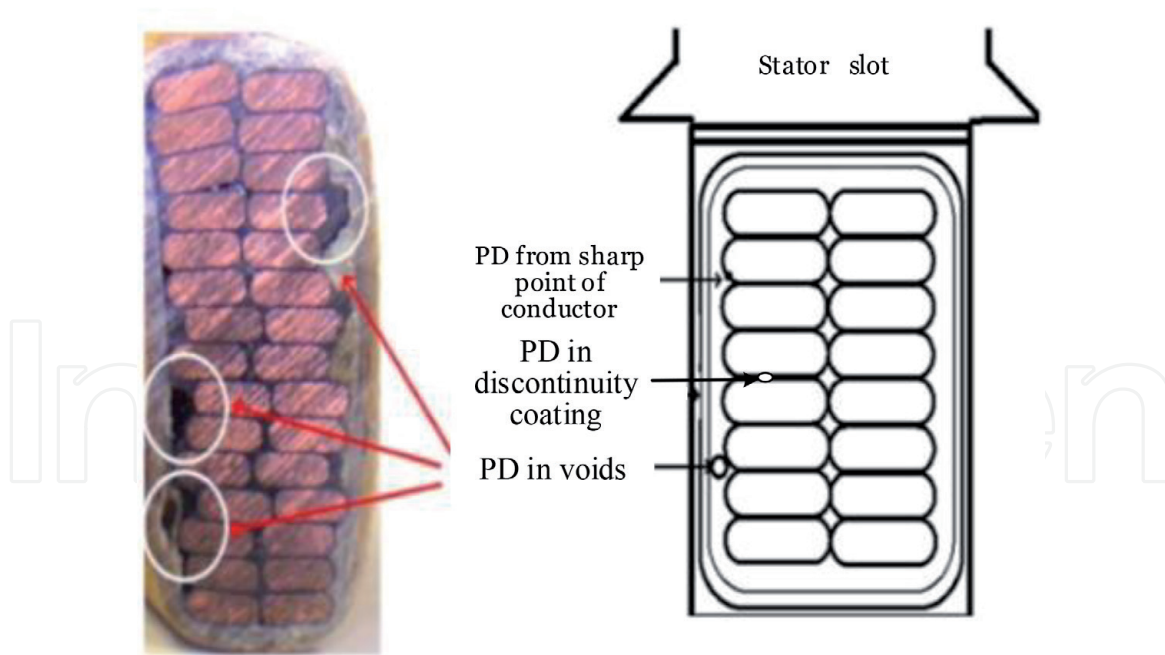*Schematic diagram and output waveform of an inverter [5].*

Figure 2.
Typical PD positions in the inner stator slot of an inter-fed motor [18].

insulation systems [15–17]. For Type II motors, formed windings are used in which the preformed coils are uniformly layered with rectangular section conductors. Form the typical cross section image of stators slot as shown in **Figure 2** [18], it can be inferred that PDs are easily occur from the sharp point of conductor, discontinuity coating, and voids formed during manufacture.

2.2 Failure mechanism under repetitive impulse voltage

Hereinafter, we will explain failure mechanism under repetitive impulse voltages though the investigation of the aging process and PD characteristics of turn-to-turn insulation of coils under repetitive impulse voltages [5]. In order to simulate the insulation structure of coils of an inverter-fed motor, the turn insulation specimens were manufactured according to the standard IEC 60034-18-42. In laboratory, bipolar repetitive square impulse voltages are used to take the place of pulse width modulated (PWM) voltage, with adjustable parameters such as amplitude, repetition frequency, and rising time. As bipolar repetitive square impulse voltages were adopted as the testing voltage, one cycle of test time is divided into 360°, and thus, we can analyze PD signals as they can be measured under AC power frequency voltage.

PD characteristics of turn insulation specimens were investigated, with the specimens be aged for 20, 60, and 100 h, respectively. Phase distribution of the discharge numbers and amplitude of PD pulses is shown in **Figure 3** [5]. Most of PD pulses appear next to the rising edge and the falling edge of square wave with a narrow distribution range from about 3 to 23° and 180 to 200°. PD pulses are rarely present during the flat region of repetitive square impulse voltages. This phase distribution characteristic is quite different from the PD characteristics under power frequency. The phase distribution appears widening tendency with the increase of aging time. Especially for the phase near 20°, the PD number and PD quantity increase obviously.

Storage effect of charges is obvious under repetitive impulse voltages. **Figure 4** [5] describes the change of space charge and electric field in the air gap at different time of bipolar continuous square impulse voltage. $E(t)$ is the applied field with electric field amplitude E_0. E_q is the electric field induced by space charge deposited
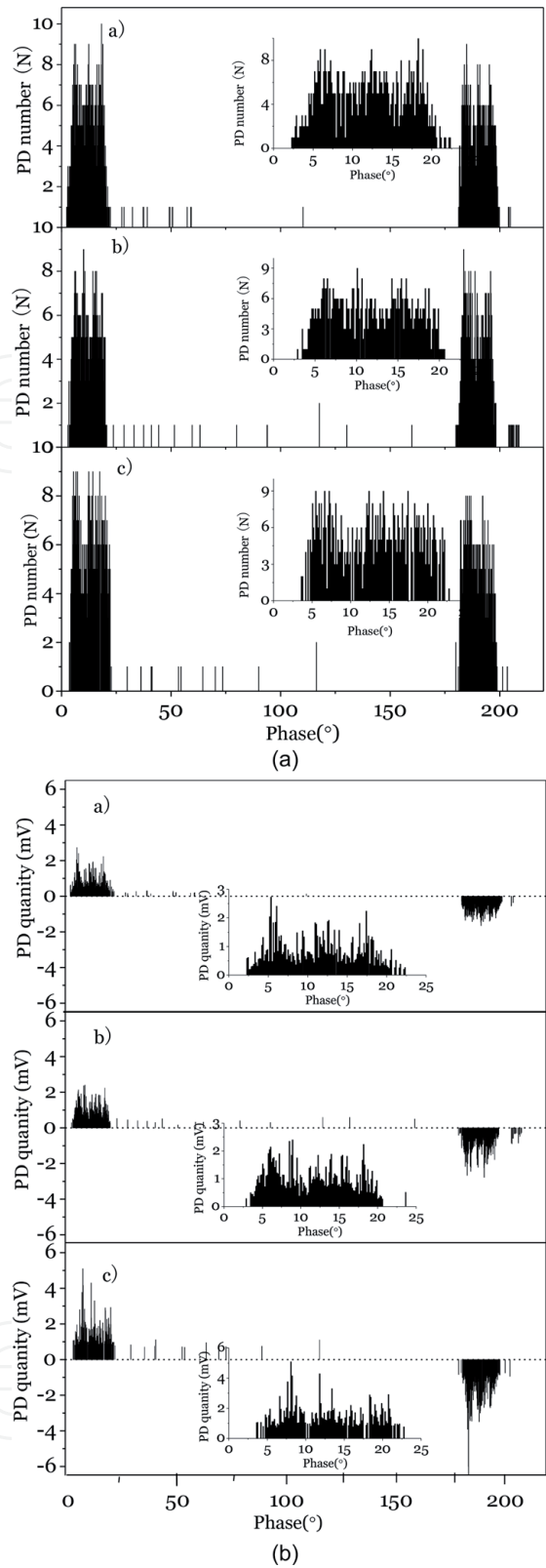
Figure 3.
PD characteristics of turn insulation specimens with different aging time. (a) Relevant phase distribution of the PD number. (b) Relevant phase distribution of PD quantity [5].

in the air gap. At the beginning, bipolar continuous square impulse voltage is applied on the sample, and the induced space charges gather in the air gap, as shown in **Figure 4a**. If the field E_i, difference between $E(t)$ and E_q, reaches PD inception field and the initiating electron is available, PD occurs, dropping the electric field E_i to a residual field value Eres = E0− Eq, as shown in **Figure 4b**. When the polarity of impulse voltage reverses, the field value in the air gap changes to Ei = −(E(t) + Eq), as shown in **Figure 4c**. Currently, space charge moves under the inverted electric
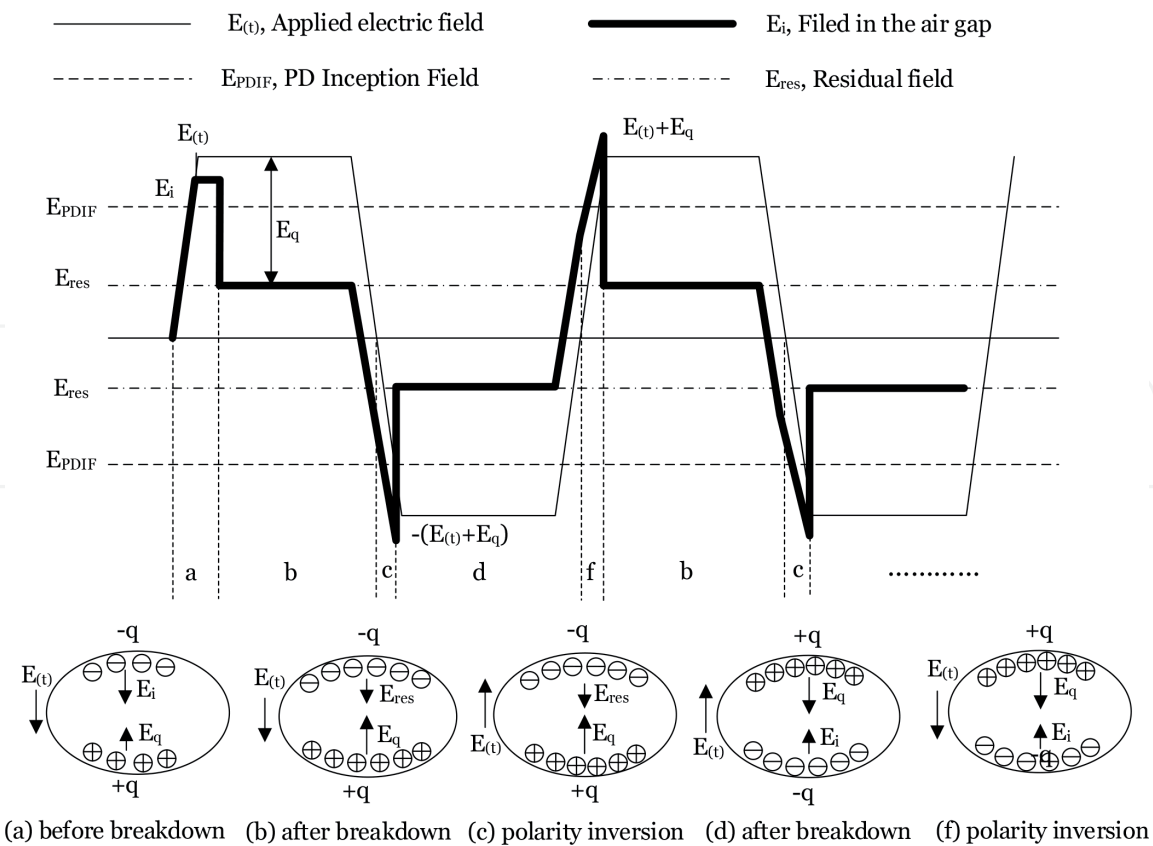
(a) before breakdown (b) after breakdown (c) polarity inversion (d) after breakdown (f) polarity inversion

Figure 4.
Storage effect of charges under repetitive impulse voltages [5].

field. But this process is very weak and most of the charge cannot perform the invert motion because of the steep front of impulse voltage. The value of E_q decreases only a little, where Eq ≈ E0-Eres. So, at the instant of polarity reverses, Ei ≈ (E(t) + E0-Eres) would be larger than PD inception field, another PD could be promoted at the falling time of bipolar continuous square impulse voltage, as shown in **Figure 4c**. The charge in the air gap completes reverse movement during the process of PD and the electric field Ei drops again to the value -Eres, as shown in **Figure 4d**. When the applied field inverse again, which is shown in **Figure 4f**, the changes of charge and electric field Ei in the air are similar with that in **Figure 4c**. PD pulse would appear again. The behavior of charge and field could repeat in succession with the testing time, which is similar with the procedures from step b to step f.

As displayed in **Figure 4**, the electric field Ei in the air gap reaches to the maximum value at the rising stage and falling stage of bipolar continuous square impulse voltage. The main reason is that the movement of charge in the air gap could not follow the polarity reversion of impulse voltage; superposition effect between applied field E(t) and the field Eq in the air gap is obvious. Consequently, Most of PDs occur during the rising edge and falling edge of continuous square impulse voltage with a narrow distribution range, which can be observed in **Figure 3**. Residual field value Eres is not constant strictly because of the dissipation of charge. Individual PD appears during the flat region of bipolar square impulse voltage when the field Ei increases to PD inception filed accidentally because of the dissipation of charge in the air gap.

Partial discharge behavior is closely related to the degree of insulation aging. During PD activities, the organic polymer is eroded and degraded gradually, which could lead to two results: first, more new voids generate, which promote the increase of PD number, and second, the original voids were enlarged because of volatilization of organics, resulting in higher PDIV. When the polarity of bipolar

continuous square impulse voltage inverses, applied voltage needs a longer delayed time to reach the higher PDIV, resulting in a higher energy of PD, which will be appear at the phase around 20° due to the time delay. This is consistent with what we discussed before that PD amplitudes and discharge numbers become higher near 20° in aged samples. Therefore, PD amplitudes and discharge numbers near 20° can be considered as critical characteristic parameters to evaluate the insulation condition under repetitive impulse voltages.

3. Property modification of polyimide films

3.1 Polyimide nanocomposites

Samples of PI/Al_2O_3 nanocomposites are usually synthetized by using in-situ polymerization. Corona-resistance lifetime under repetitive impulse voltages for nanocomposites with different content of Al_2O_3 nanofillers is investigated. And then, the effects of nanoparticles on reducing the degradation of polyimide nanocomposites will be analyzed in this section.

3.1.1 Lifetime under repetitive impulse voltages for polyimide nanocomposites

During lifetime measurement under repetitive impulse voltages, PDs occur in the air gap between the film sample and the upper rod electrode. PDs generate high-energy electron, ultraviolet rays, and high activity chemical groups, which would accelerate the insulation material aging [19, 20]. Reaching the lifetime, the failure of polymer nanocomposites would occur due to the fracture and degradation of the polymer chains [21].

As shown in **Figure 5** [22], the lifetime increases with the increasing nano-Al_2O_3 content. For the PI/Al_2O_3 nanocomposites with 25 wt.% content of nano-Al_2O_3, the lifetime is around 136 h, which is about 23 times longer than that of pure PI film, at
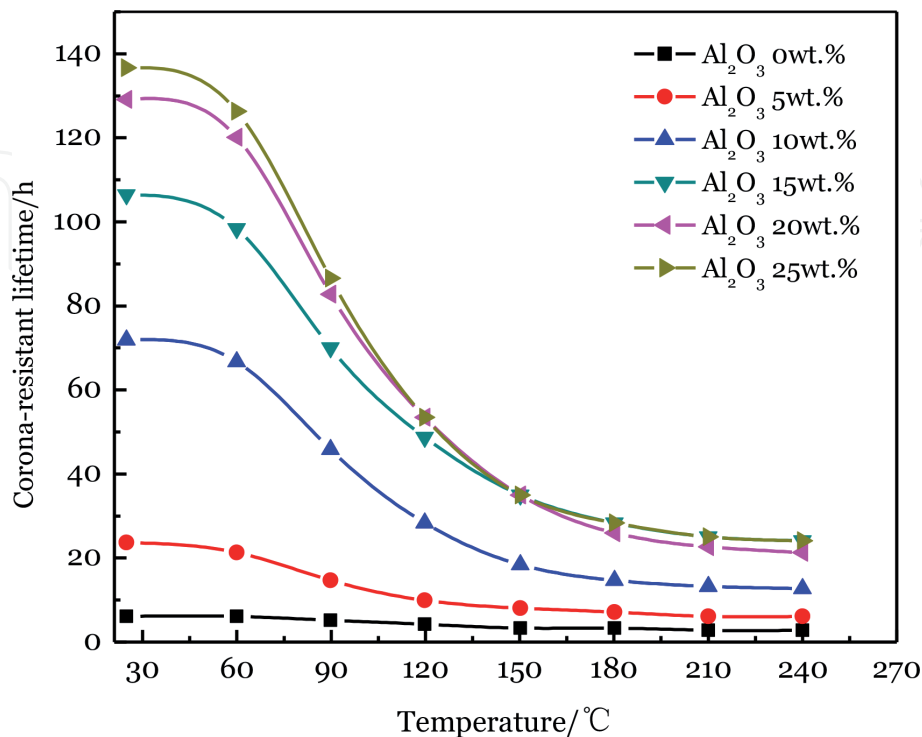

Figure 5.
Lifetime under repetitive impulse voltages of PI/Al_2O_3 nanocomposites [22].

the temperature of 25°C. Besides, the lifetime of PI/Al$_2$O$_3$ nanocomposites exhibits the obvious temperature dependence, which decreases gradually with increasing temperature. With increasing nano-Al$_2$O$_3$ content, the temperature dependence is much stronger.

3.1.2 Effects of nanoparticles on reducing the degradation of polyimide nanocomposites

The effects of nanoparticles on reducing the degradation of polyimide nano-composites can be deriving from the following three aspects.

First, during the lifetime measurement under repetitive impulse voltages, PD-induced degradation of the polymer chains occurs. With higher melting point, inorganic particles would leave on the film surface, acting as obstacles in the erosion path of polyimide matrix. Then, the degradation of polymer matrix can be reduced, resulting in a prolonged lifetime. This statement can be proved through the element distribution analysis around the breakdown point, as shown in **Figure 6** and **Table 1** [23]. Next to the breakdown point, the mass percentage of Al is almost twice higher than the mean content (2.65%) in PI/Al$_2$O$_3$ nanocomposites with Al$_2$O$_3$ content of 5 wt.%. This is consistent with the statement that inorganic particles left on the surface of eroded regions.

Second, new chemistry bonds would be generated in the interfacial regions of polyimide nanocomposites, which is the lowest bonding energy. Under the effect of PDs, these weak bonds would be broken first, followed by the ether linkage, imide ring and aromatic ring of polyimide matrix, as shown in **Figure 7** [23].
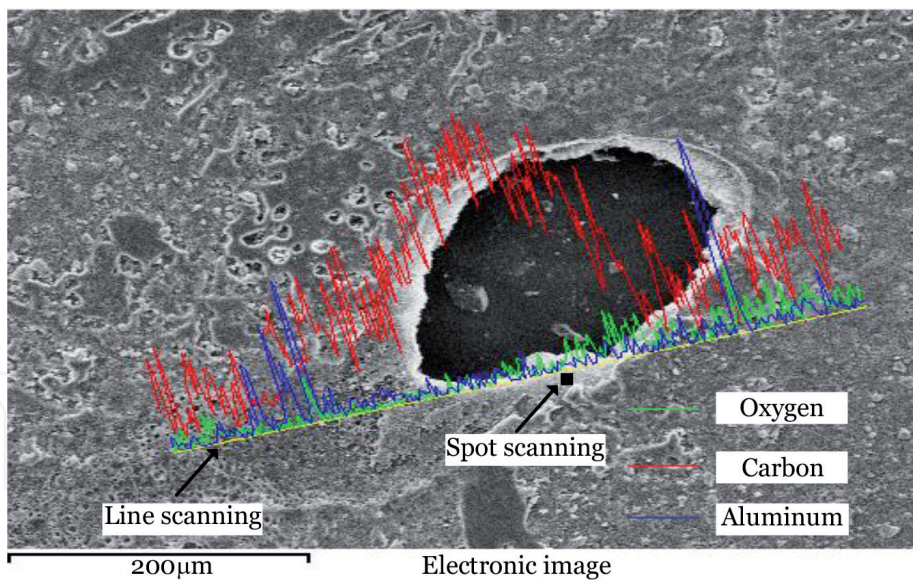

Figure 6.
EDS of spot and line scanning around the breakdown point of PI/Al$_2$O$_3$ nanocomposites with Al$_2$O$_3$ content of 5 wt.% [23].

Element	Spot scanning (Mass %)	Line scanning (Mass %)
Carbon	30.61	29.70
Oxygen	65.65	57.27
Aluminum	5.74	13.03

Table 1.
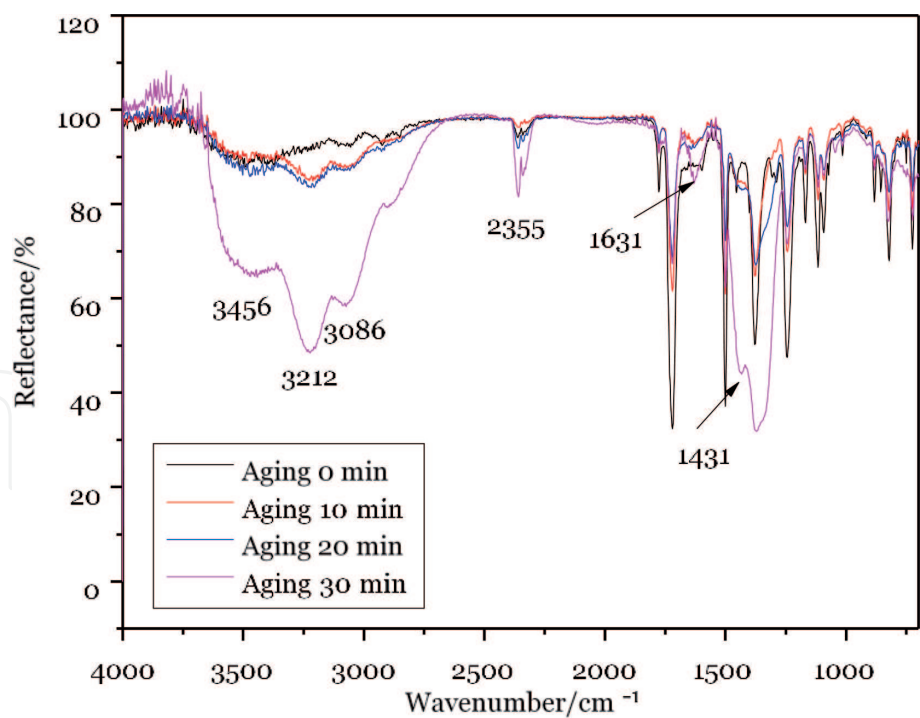*Mass percentage of elements in EDS result [23].*

Figure 7.
FTIR spectrums of PI and PI/Al$_2$O$_3$ nanocomposites (5 wt.%) at different aging time [23].
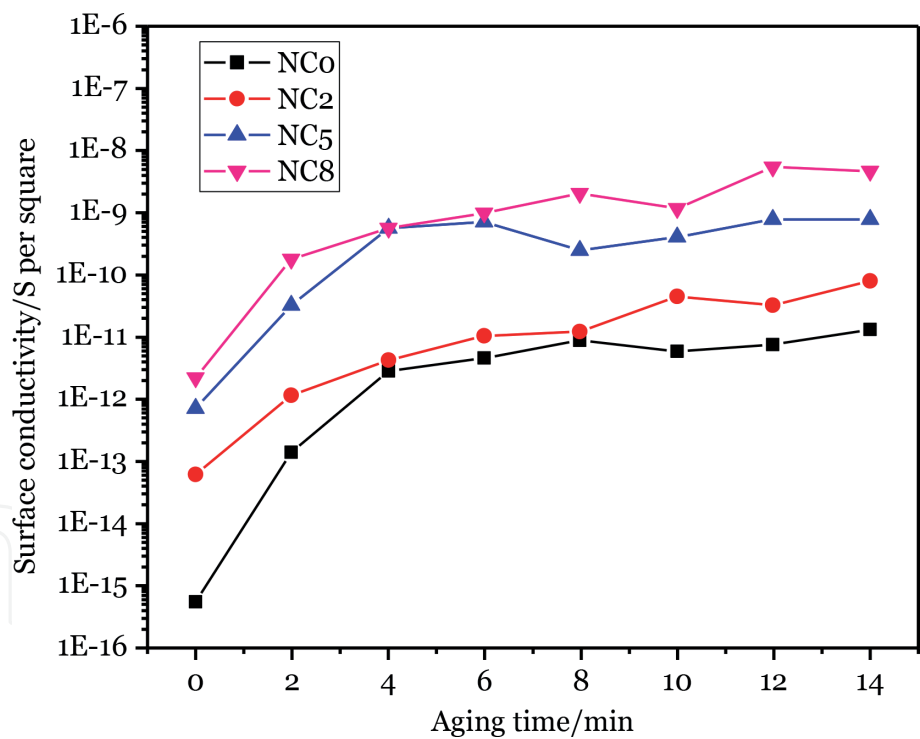

Figure 8.
Surface conductivity of PI and PI/Al$_2$O$_3$ nanocomposites [23].

Thus, weakest bonds in interfacial regions would be destroyed at the first stage of aging, which helped reduce the dissociations of other chemical bonds of polyimide molecules, by absorbing part of PD energy, resulting in a prolonged lifetime.

Third, surface conductivity of polyimide nanocomposites is higher than that of polyimide matrix, as shown in **Figure 8** [23], which facilitates surface charge dissipation, leading to lower PD intensity, and longer lifetime. The inorganic particles and the interfacial region near the film surface, with higher carrier
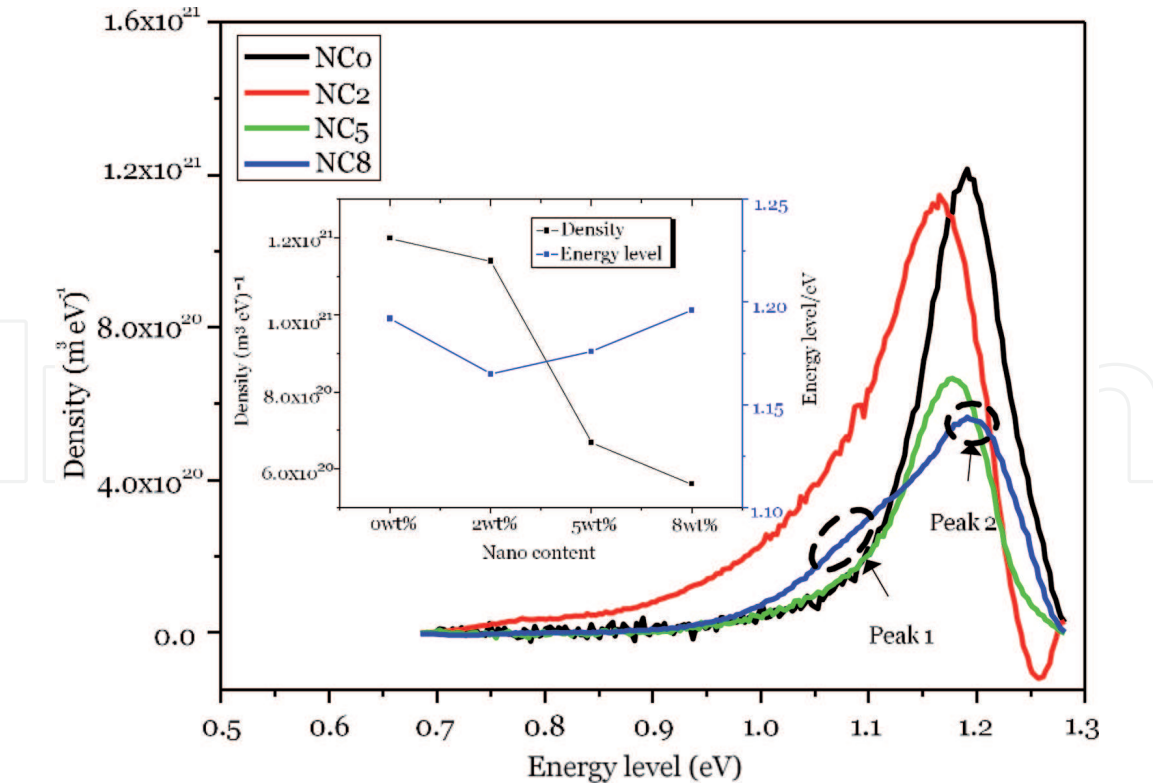
Figure 9.
Trap energy and density distributions of PI and PI/Al$_2$O$_3$ nanocomposites [23].

transfer ability, are mainly responsible for the increase in surface conductivity of polyimide nanocomposites. Improved surface conductivity can facilitate charge dissipation and mitigates the electric field distortion, resulting in higher PDIV and longer lifetime.

At last, dielectric characteristics of polyimide nanocomposites are greatly influenced by different trap density and energy distributions which depend on physical and chemical defects in dielectrics. As to deep traps, named as peak 2 in **Figure 9** [23], the trap energy nearly changes for polyimide nanocomposites, but trap density declines with increasing nanoparticle concentration, which means that the bonds between nanoparticles and polyimide molecules can restrict the movement of molecular and thus reduce the chemical disorder.

Besides, shallower traps are introduced in nanocomposites as nanocomposites content increases, as peak 1 appears on the curve of polyimide nanocomposites. With lower trap density, it is less possible for charge recombination in polyimide nanocomposites, thus lead to lower released energy, which is beneficial to reduce the degradation of polymer.

Many chemical defects are generated during PD aging due to the breakage of long molecular chain, which are reflected on the increase of both trap density and energy level. As the degree of electrical aging can be determined by the rate of increase in the density of stress-created traps [24], it can be concluded that the degree of PD aging is quite serious in PI after aging for 15 min, while that of PI/Al$_2$O$_3$ nanocomposites is much slighter. That is why no obvious increase trend can be observed in the trap density when the PD aging time is less than 15 min.

Besides, the trap-level distribution showed that both trap density and energy in PI/Al$_2$O$_3$ nanocomposites decreased as degradation, while the trend of PI was opposite. It indicated that the degradation of PI/Al$_2$O$_3$ nanocomposites was mitigated compared with PI, which could be attributed to the improved electrical characteristics of PI/Al$_2$O$_3$ nanocomposites.

3.2 Surface modification of polyimide films

Non-thermal plasma generated by dielectric barrier discharge (DBD) can be used to conduct surface modification of polyimide films [25]. This kind of plasma modification can efficiently cause the material surface cross-linking, etching, and the introduction of polar groups, without changing its bulk properties. Surface modification of polymer films using DBD are usually conducted to improve adhesion or hydrophilicity properties, as DBD exited high-energy electrons produce ions and reactive species that interact with film surface to modify the surface characteristics. Electrical properties such as surface flashover voltage and surface resistivity can also be improved by non-thermal plasma modification [26–28].

In this section, we will study lifetime improvement and its mechanism under repetitive impulse voltages, by considering the influence of trap energy distribution on carrier transportation and charge dissipation with voltage reversion. Thus, isothermal surface potential decay (ISPD) [29, 30] technique was conducted to study the charge transport characteristics of PI films before and after surface modification, revealing the energy distribution of both electron-type and hole-type traps [31].

3.2.1 Properties of plasma-modified polyimide films

Polyimide films were put between the air gap of DBD for surface modification, with different treating time set as 0, 10, 20, 30, 60, and 90 s. The DBD was excited by non-thermal plasma generator in atmospheric air, as shown in **Figure 10**.

The surface of the polyimide films was etched during plasma treatment. As shown in **Figure 11**, embossing, micro-voids, and obvious etched channels gradually appear on film surface, with increasing treating time. Based on the energy disperse spectroscopy (EDS) analysis results shown in **Table 2**, it is indicated that the oxygen content of plasma-treated films is higher than that of untreated film. This would be attributed to the introduction of rich-oxygen groups onto the film surface during plasma treatment.
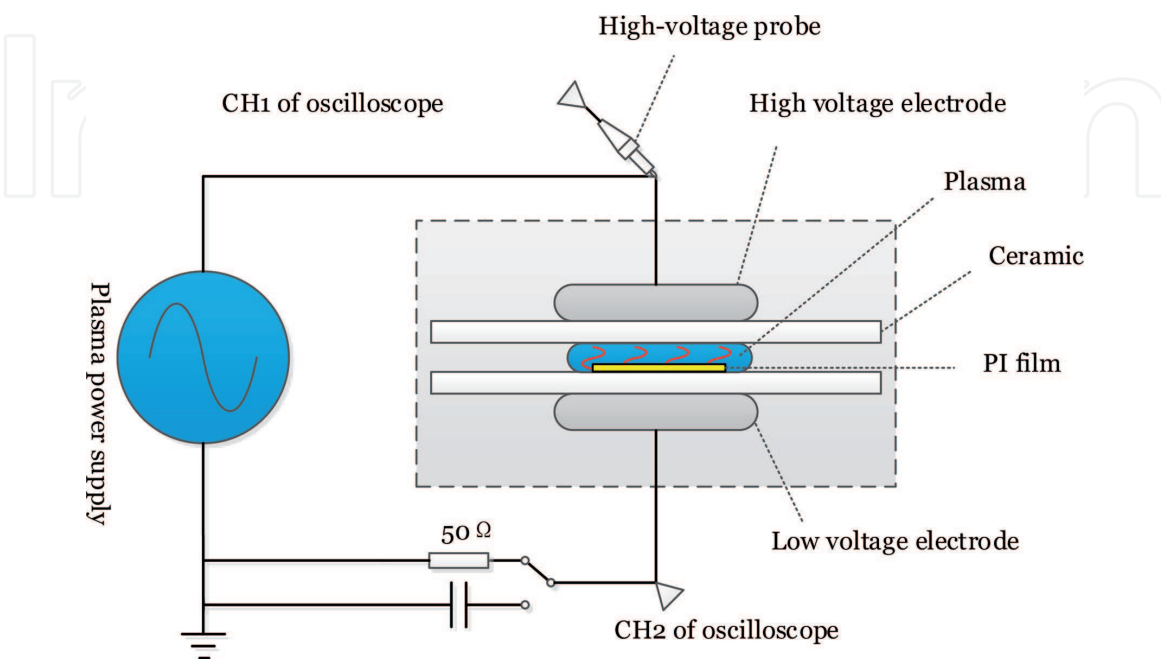

Figure 10.
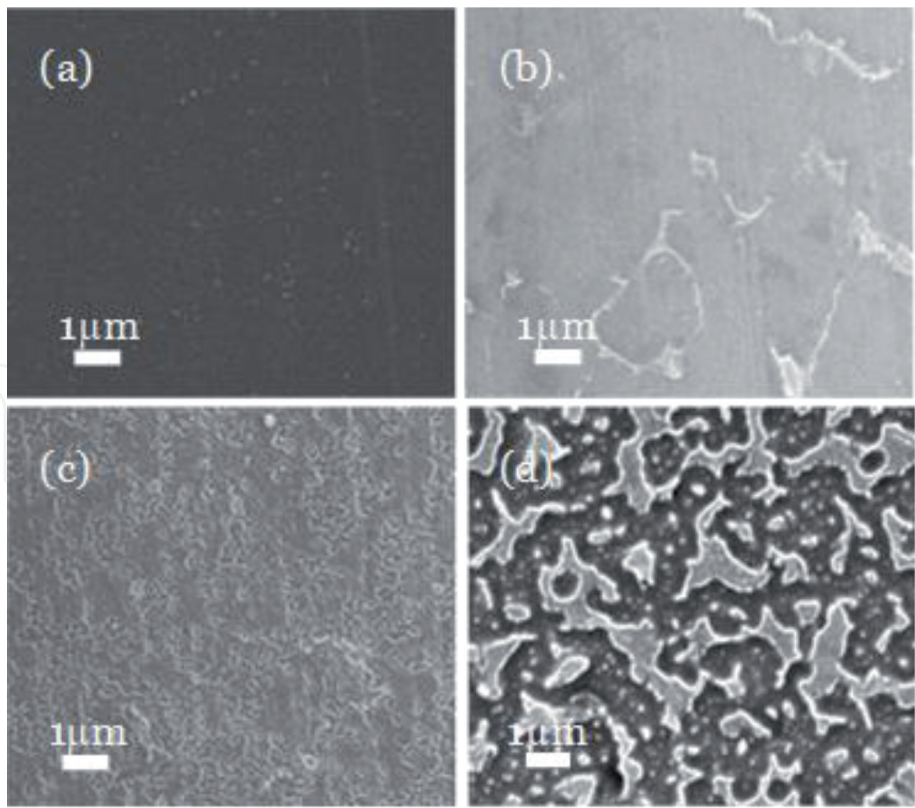*Setup for dielectric barrier discharge (DBD) plasma treatment.*

Figure 11.
SEM images of PI after different treating time. (a) PI. (b) PI-20. (c)PI-30. (d) PI-90.

| Samples	Weight percentage of C (wt %)	Weight percentage of O (wt %)
PI	21.71	78.29
PI-90	18.70	81.30

Table 2.
Elemental analysis of PI films before and after plasma treatment.

Main molecular chains of PI have not been changed by plasma treatment [32, 33], while the intensities of these characteristic absorption peaks for plasma-treated films obviously decrease compared with untreated films, indicating some ring-opening reactions occurred during plasma treatment, as shown in **Figure 12**. Moreover, absorption bands between 3660 and 3200 cm^{-1}, which represent O—H stretching peaks in carboxyl acids [32, 33], can be observed in plasma-treated films. Peaks appear at 1410(—COOH) and 3220(—NH2) cm^{-1} also increase in plasma-treated films, indicating that reactive species, containing oxygen and nitrogen, have been introduced onto the film surface during plasma treatment. However, when the treating time is longer than 30 s, the intensities of characteristic absorption peaks representing —COOH and —NH2 obviously decrease. This would be attributed to further oxidizing reactions during plasma treatment, as working gas is air. Thus, appropriate treating time is an important factor to introduce reactive groups effectively.

Lifetime under repetitive impulse voltage for plasma-treated films can be improved when the plasma treating time is less than 20 s, but it decreases with increasing treating time, when the treating time is longer than 20 s, as shown in **Figure 13**. When the treating time is 20s, the lifetime reaches the maximum value of 23.5 min, which is 16.9% higher than that of untreated samples. When the treating time exceeds 30 s, the lifetime decreases sharply, by reaching the values even shorter than that of untreated samples.
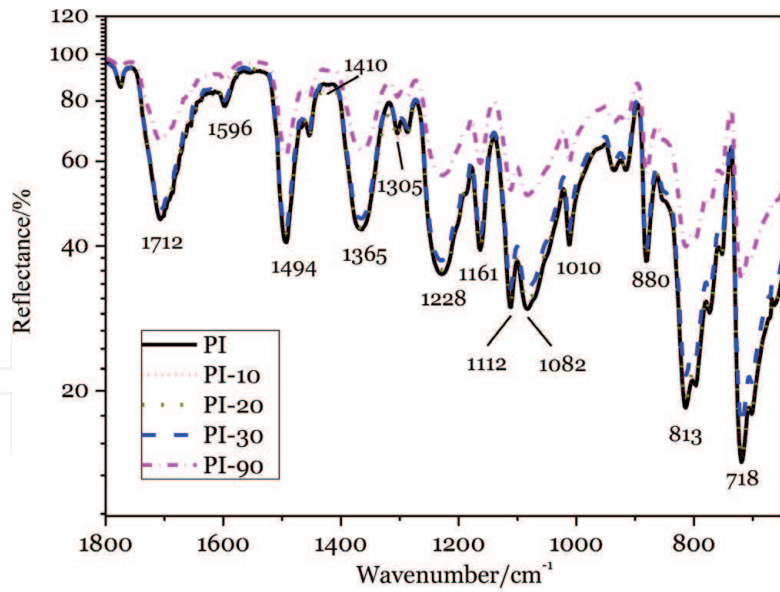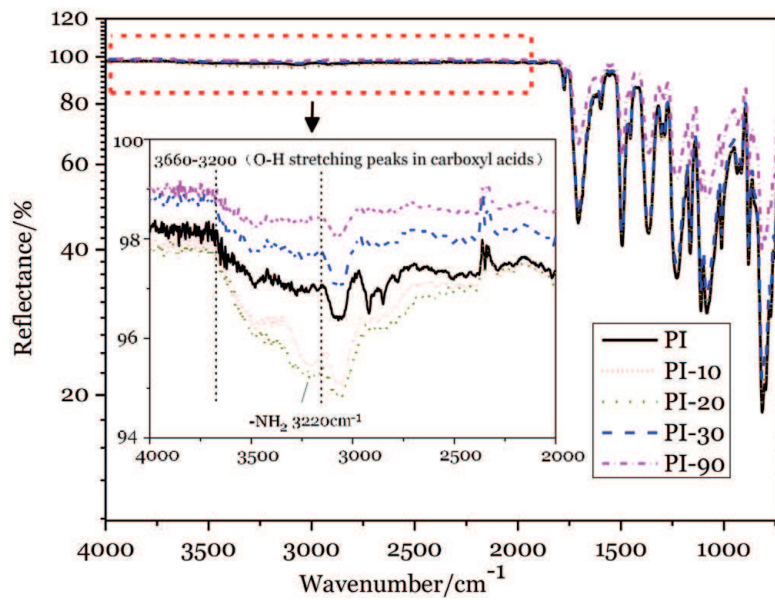
Figure 12.
FTIR spectra of PI films under different plasma treating time. (a) 1800–700 cm^{-1}. (b) 4000–700 cm^{-1}.

3.2.2 Modification mechanism

The energy levels of both electron-type and hole-type traps are lower in plasma-treated films than that in untreated ones, as shown in **Figure 14**. Apparent decrease of trap energies takes place when the treating time is shorter than 20 s. However, the trap energy levels increase when the treating time exceeds 20 s, but they are still lower than that of untreated samples. For each curve, two peaks can be observed, which represent the distribution of shallow and deep traps, respectively.

Shallow trap energy level for PI-20 is the lowest compared with the others, corresponding to the longest lifetime repetitive impulse voltages. Trap energy level dominates charge transfer characteristics rather than trap density. With lower shallow trap energy level, carriers are easier to transfer through the sample, causing less charge accumulation. For deeper traps, more energy is needed to detrap the carriers, which means more charges are trapped in samples. Only the near surface region with the depth about ~90 nm of the material has been modified by reactive
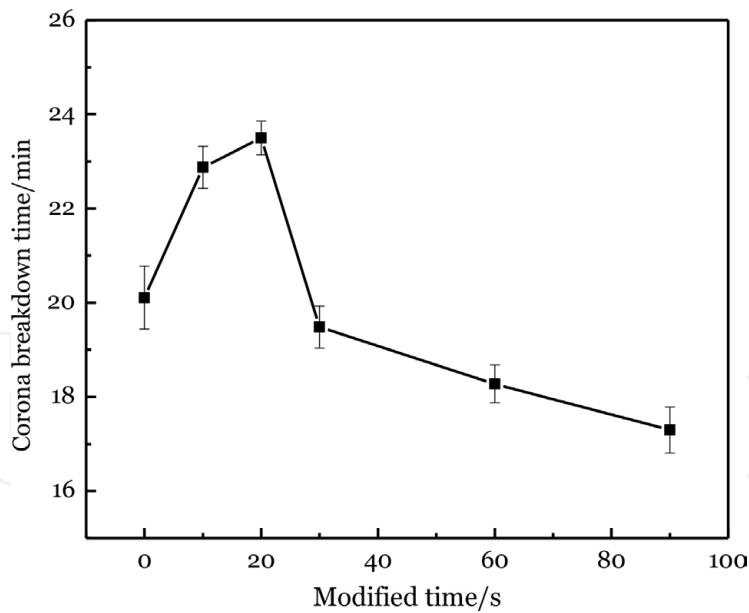
Figure 13.
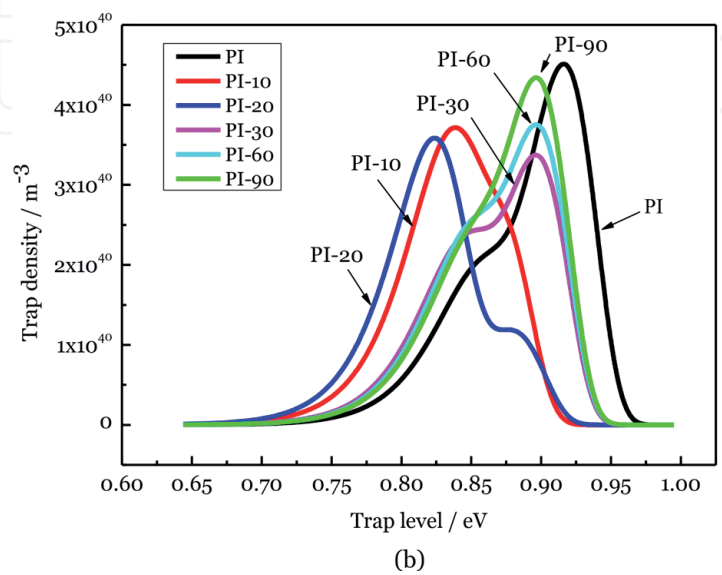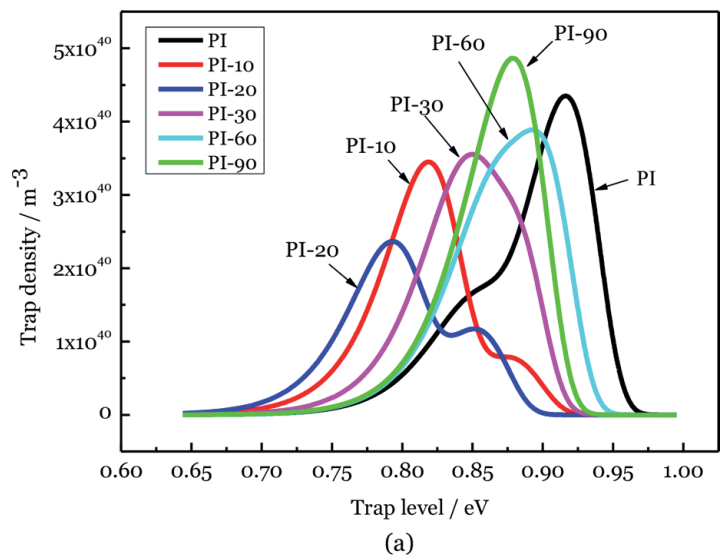*Lifetime under repetitive impulse voltage with different plasma treating time.*

Figure 14.
Trap energy distribution of PI films under different treating time. (a) Energy distribution of hole-type traps.
(b) Energy distribution of electron-type traps.

13

groups during plasma treatment [34]. Thus, the trap distribution modification mainly occurs in the near surface region, by introducing groups contained oxygen and nitrogen. Corresponding charge transportation and accumulation characteristics modification also takes place in this near surface region. When it comes to the repetitive impulse voltages, the trapped surface charges will be superposed to the applied voltage as polarity reverses, and local field would be further enhanced [23]. In this case, lifetime will be shortened due to intensive PD activity. For plasma-treated films, with lower energies of both shallow and deep traps, charge dissipation would be enhanced and the density of trapped charges would be reduced, leading to the local electric filed mitigation, resulting in suppressed PD intensity and corresponding longer lifetime.

However, when the treating time is too long, plasma-introduced oxygen and nitrogen rich groups would be broken by further oxidizing reactions, so less effective active groups have been introduced through plasma treatment. Furthermore, the degradation of PI films begins to occur, which means large molecular chains of PI began to break. It is more likely to form low-density region on the film surface. Although the charge dissipation is enhanced by the effect of shallower traps and corresponding PD activity might be weakened, this low-density region still cannot withstand the weakened PD intensity, and cleavages of the molecular chain will take place subsequently. Finally, the dielectric breakdown will occur in a short time.

4. Conclusion

The insulation system of inverter-fed motors is subjected to repetitive impulse voltages which are generated by pulse width modulation (PWM) converters. The insulation materials are expected to withstand partial discharge (PD) activity during service. Under repetitive impulse voltages, most of PD pulses appear next to the rising edge and the falling edge of applied voltage but rarely present during the flat region of repetitive square impulse voltages, which is quite different from the PD characteristics under power frequency. The phase distribution appears widening tendency with the increase of aging time. Especially for the phase near 20°, the PD number and PD quantity increase obviously.

As turn-to-turn insulation of inverter-fed traction motors, the dielectric properties of polyimide need to be improved to meet the requirement for rapid development of industry application, especially for PD-dependent lifetime under repetitive impulse voltages. Lifetime under repetitive impulse voltages can be improved by synthesizing polyimide/inorganic nanocomposites and plasma treatment.

For polyimide nanocomposites, during degradation process, inorganic particles would leave on the film surface of polyimide due to higher melting point, acting as obstacles in the erosion path of polyimide matrix. New chemistry bonds would be generated in the interfacial regions of polyimide nanocomposites, which is the lowest bonding energy. These weak bonds would be destroyed at the first stage of aging, reducing dissociations of other chemical bonds of polyimide molecules. With improved surface conductivity, charge dissipation of polyimide nanocomposites mitigates the electric field distortion, resulting in higher PDIV. As shallower traps are introduced in nanocomposites, it is less possible for charge recombination in polyimide nanocomposites, leading to lower released energy, which is beneficial to reduce the degradation of polymer.

For plasma-treated films, lower shallow trap energy level is beneficial to charge transfer; with lower deep trap energy level, less charge accumulation takes place. Trap energy level dominates the charge transportation and accumulation characteristics rather than trap density. Active groups contained oxygen and nitrogen, which

are introduced during plasma treatment, are responsible for trap energy distribution modification of PI films. Under repetitive impulse voltage, faster surface potential decay rate and less charge accumulation can facilitate charge dissipation and local electric field mitigation, resulting in weakened PD intensity and a longer lifetime. Appropriate treating time is an important factor to introduce reactive groups and prolong the lifetime.

Acknowledgements

Author details

Yan Yang* and Guangning Wu
School of Electrical Engineering, Southwest JiaotongUniversity, China

*Address all correspondence to: yangyanyy@swjtu.edu.cn

IntechOpen

References

[1] Zhou L, Wu G, Gao B, et al. Study on charge transport mechanism and space charge characteristics of polyimide films. IEEE Transactions on Dielectrics and Electrical Insulation. 2009;**16**(4):1143-1149

[2] Hayakawa N. Partial discharge characteristics of inverter-fed motor coil samples under ac and surge voltage conditions. IEEE Electrical Insulation Magazine. 2005;**21**(1):5-10

[3] Kandev N, Castelan P, Lebey T, et al. Testing of low-voltage motor turn insulation intended for pulse-width modulated applications. IEEE Transactions on Dielectrics and Electrical Insulation. 2000;**7**(6):783-789

[4] Yin W. Failure mechanism of winding insulations in inverter-fed motors. IEEE Electrical Insulation Magazine. 1997;**13**(6):18-23

[5] Luo Y, Wu G, Liu J, et al. PD characteristics and microscopic analysis of polyimide film used as turn insulation in inverter-fed motor. IEEE Transactions on Dielectrics and Electrical Insulation. 2014;**21**(5):2237-2244

[6] Kaufhold M, Aninger H, Berth M, et al. Electrical stress and failure mechanism of the winding insulation in PWM-inverter-fed low-voltage induction motors. IEEE Transactions on Industrial Electronics. 2000;**47**(2):396-402

[7] Akram S, Wu G, Gao GQ, et al. Cavity and interface effect of PI-film on charge accumulation and PD activity under bipolar pulse voltage. Journal of Electrical Engineering and Technology. 2015;**10**(5):2089-2098

[8] Nehete K, Sharma RA, Chaudhari L, et al. Study of erosion resistance and mechanical properties of unsaturated polyester based nano-composites. IEEE Transactions on Dielectrics and Electrical Insulation. 2012;**19**(2):373-382

[9] Li Z, Okamoto K, Ohki Y, et al. Effects of nano-filler addition on partial discharge resistance and dielectric breakdown strength of micro-Al2O3/epoxy composite. IEEE Transactions on Dielectrics and Electrical Insulation. 2010;**17**(3):653-661

[10] Tanaka T, Ohki Y, Ochi M, et al. Enhanced partial discharge resistance of epoxy/clay nanocomposite prepared by newly developed organic modification and solubilization methods. IEEE Transactions on Dielectrics and Electrical Insulation. 2008;**15**(1):81-89

[11] Maity P, Basu S, Parameswaran V, et al. Degradation of polymer dielectrics with nanometric metal-oxide fillers due to surface discharges. IEEE Transactions on Dielectrics and Electrical Insulation. 2008;**15**(1):52-62

[12] Kwon OJ, Tang S, Myung SW, et al. Surface characteristics of polypropylene film treated by an atmospheric pressure plasma. Surface and Coatings Technology. 2005;**192**(1):1-10

[13] Park WJ, Yoon SG, Jung WS, et al. Effect of dielectric barrier discharge on surface modification characteristics of polyimide film. Surface & Coatings Technology. 2007;**201**(9):5017-5020

[14] Kostov KG, Nishime TMC, Hein LRO, et al. Study of polypropylene surface modification by air dielectric barrier discharge operated at two different frequencies. Surface and Coatings Technology. 2013;**234**:60-66

[15] Persson E. Transient effects in application of PWM inverters to induction motors. IEEE Transactions on Industry Applications. 2002;**28**(5):1095-1101

[16] Stone GC, Van Heeswijk RG, Bartnikas R. Investigation of the effect of repetitive voltage surges on epoxy insulation. IEEE Transactions on Energy Conversion. 1992;**7**(4):754-760

[17] Wheeler JCG. Effects of converter pulses on the electrical insulation in low and medium voltage motors. IEEE Electrical Insulation Magazine. 2005;**21**(2):22-29

[18] Wang P, Wu G, et al. Study of partial discharge characteristics at repetitive square voltages based on UHF method. Science China Technological Sciences. 2013;**56**(1):262-270

[19] Morshuis PHF. Degradation of solid dielectrics due to internal partial discharge: Some thoughts on Progress made and where to go now. IEEE Transactions on Dielectrics and Electrical Insulation. 2005;**12**(5):905-913

[20] Mayoux C. Degradation of insulating materials under electrical stress. IEEE Transactions on Dielectrics and Electrical Insulation. 2000;**7**(5):590-601

[21] Zhu Y, Otsubo M, Honda C. Degradation of polymeric materials exposed to corona discharges. Polymer Testing. 2006;**25**(3):313-317

[22] Luo Y, Wu G, Liu J, et al. Investigation of temperature effects on voltage endurance for polyimide/Al2O3 nanodielectrics. IEEE Transactions on Dielectrics and Electrical Insulation. 2014;**21**(4):1824-1834

[23] Zhong X, Wu G, Yang Y, et al. Effects of nanoparticles on reducing partial discharge induced degradation of polyimide/Al2O3 nanocomposites. IEEE Transactions on Dielectrics and Electrical Insulation. 2018;**25**(2):594-602

[24] Liufu D, Wang X, Tu D, et al. High-field induced electrical aging in polypropylene films. Journal of Applied Physics. 1998;**83**(4):2209-2214

[25] Shao T, Zhang C, Long K, et al. Surface modification of polyimide films using unipolar nanosecond-pulse DBD in atmospheric air. Applied Surface Science. 2010;**256**(12):3888-3894

[26] Shao T, Yang W, Zhang C, et al. Enhanced surface flashover strength in vacuum of polymethylmethacrylate by surface modification using atmospheric-pressure dielectric barrier discharge. Applied Physics Letters. 2014;**105**(7):082903-082264

[27] Shao T, Liu F, Hai B, et al. Surface modification of epoxy using an atmospheric pressure dielectric barrier discharge to accelerate surface charge dissipation. IEEE Transactions on Dielectrics and Electrical Insulation. 2017;**24**(3):1557-1565

[28] Zhao W, Xu R, Ren C, et al. Ion-implantation modification of surface flashover properties in vacuum of polytetrafluoroethylene. IEEE Transactions on Plasma Science. 2018:1-7

[29] Li J, Zhou F, Min D, et al. The energy distribution of trapped charges in polymers based on isothermal surface potential decay model. IEEE Transactions on Dielectrics and Electrical Insulation. 2015;**22**(3):1723-1732

[30] Min D, Cho M, Khan AR, et al. Surface and volume charge transport properties of polyimide revealed by surface potential decay with genetic algorithm. IEEE Transactions on Dielectrics and Electrical Insulation. 2012;**19**(2):600-608

[31] Han Y, Li S, Min D. Trap energy distribution in polymeric insulating materials through surface potential decay method. IEEE Transactions on Dielectrics and Electrical Insulation. 2018;**25**(2):639-648

[32] Park SJ, Lee HY. Effect of atmospheric-pressure plasma on adhesion characteristics of polyimide film. Journal of Colloid and Interface Science. 2005;**285**(1):267-272

[33] Yang Y, Yin D, Xiong R, et al. Ftir and dielectric studies of electrical aging in polyimide under AC voltage. IEEE Transactions on Dielectrics and Electrical Insulation. 2012;**19**(2):574-581

[34] Park B, Kim J, Cho M, et al. Ballistic-mode plasma-based ion implantation for surface-resistivity modification of polyimide film. IEEE Transactions on Plasma Science. 2012;**40**(6):1749-1752